ACS OMEGA

http://pubs.acs.org/journal/acsodf

Mini-Review

# Antibacterial Efficacies of Nanostructured Aminoglycosides

Smritilekha Bera* and Dhananjoy Mondal

Cite This: *ACS Omega* 2022, 7, 4724−4734

Read Online

ACCESS | Metrics & More | Article Recommendations | Supporting Information

**ABSTRACT:** The widespread use of broad-spectrum aminoglycoside antibiotics is restricted from various clinical applications due to the emergence of bacterial resistance and the adverse effects such as ototoxicity and nephrotoxicity. The intensive applicability of nanoparticles in modern medicinal chemistry has gained the interest of researchers for modification of aminoglycosides as nanoconjugates either via covalent conjugation or physical interactions to alleviate their undesirable effects and bacterial resistance. In this context, various carbohydrates, polymers, lipids, silver, gold, and silica-attached aminoglycoside nanoparticles have been reported with improvements in physicochemical properties, bioavailability, and biocompatibility in physiological medium. Overall, this review encompassed the synthesis of nanostructured aminoglycosides and their applications in the development of new antibacterial therapeutics.

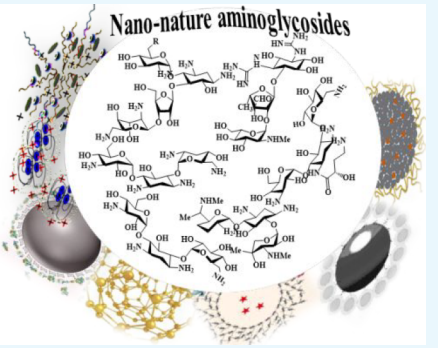


## 1. INTRODUCTION

Nanoscience and its associated technology represent revolutionary research in drug manufacturing, particularly, diagnostics, imaging, and/or drug delivery at the cellular or atomic level. The discoveries mainly focus on the enhancement of drug specificity to cells, the efficacy of targeted drug delivery, and suitability of carriers for drug distribution and drug toxicity reduction. The unique and well-defined pharmacodynamic and pharmacokinetic properties of nanomaterials[1] result from the effects of ultrasmall and well-behaved quantum size, large surface by volume ratio, shape, functionalized structure, surface charge, and unusual electrodynamic interactions with the biological system, among other parameters. Likewise, the tunable physicochemical properties of nanoparticles in addition to crystallinity, electronic states, surface instability, surface roughness, and radius of curvature contribute in different ways to greatly affect their medicinal properties. In this regard, we understand from the literature that nanostructured materials encourage the delivery of drugs to a preferred site of action in the living organism, overcoming biological barriers such as the blood−brain barrier as well as intestinal, nasal, pulmonary, and skin barriers.[2] Even though the involvement of nanostructure materials in different areas is well-recognized, the participation in the field of antimicrobials is highly significant. Well-known clinically used broad-spectrum bactericidal aminoglycoside antibiotics (AAs) are active against aerobic Gram-negative as well as a few Gram-positive microorganisms (Figure 1a) and are used to treat opportunistic infections with AIDS, cystic fibrosis, and cancer. Unfortunately, the extensive use of these aminoglycosides is impeded by significant dose-related toxicities, poor adsorption in the gastrointestinal tract (GIT), low solubility and permeability into the bacterial cell membrane, as well as the rapid rise of AA-resistant strains around the world. The looming threat of aminoglycoside resistance emerges because of enzymatic hydrolysis, target site modification, impaired entry to the bacterial cell, and active AA efflux. Furthermore, the global market for aminoglycosides was assessed at more than 1.1 billion USD in 2014, and it is predicted to grow at a CAGR (compound annual growth rate) of more than 3.0% in the coming years, owing to the rising prevalence of bacterial infections affected by Gram-positive and Gram-negative bacteria (Figure 1B). Thus, access to aminoglycosides in a new state with antibacterial activity, low toxicity, and smaller susceptibility to aminoglycoside-modifying enzymes compared to those of their parent structures is required.

From a structural perspective, aminoglycosides are polycationic pseudo-oligosaccharides with an aminocyclitol/streptamine core linked to an aminated sugar. The primary binding sites of AAs are the hydroxy and amino groups, which engage in interaction with the A-site decoding area of the bacterial 16S rRNA, causing cell death by inhibiting protein synthesis. These groups are responsible for high-water solubility and limited lipid solubility, in addition to their easy synthetic modification. Several synthetic approaches to find the next generation of AAs with improved biological and therapeutic functions have been articulated mainly, fostering their uptake property modification or enzymatic alteration for the mechanistic studies toward the resistance of AAs with different multi-drug-resistant bacteria.[3]

**Received:** August 14, 2021
**Accepted:** January 18, 2022
**Published:** February 6, 2022





https://doi.org/10.1021/acsomega.1c04399
*ACS Omega* 2022, 7, 4724−4734

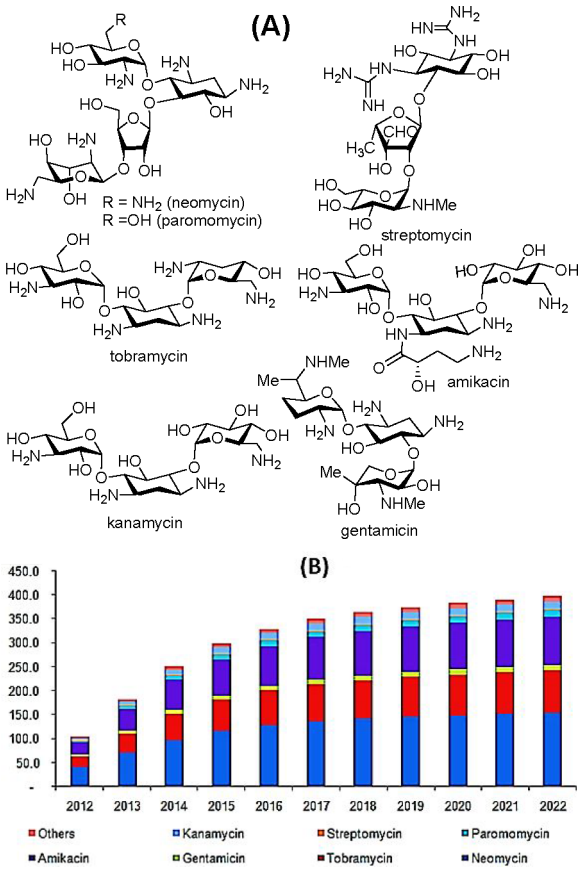


**Figure 1.** (A) Aminoglycoside antibiotics. (B) Uses of aminoglycosides in North America between 2012 and 22 (millions in USD) (www.grandviewresearch.com/industry-analysis/aminoglycoside-market).

The benefits of current nanomedicine in an aspect of pharmacokinetic and pharmacodynamic characteristics could lead to more effective actions.[4] We have witnessed the unique and customizable features of nanomaterials that make the drugs easier to administer, eliminating some shortcomings of traditional antibiotic therapies. Thus, the use of nanomedicine and its associated technology could modify the existing aminoglycosides to yield nanostructured aminoglycosides for addressing the above-mentioned limitations of AAs. In this review article, the synthesis and applications of nanostructured AAs are presented.

## 2. SYNTHESIS OF NANOSTRUCTURED AMINOGLYCOSIDES

For the synthesis of nanostructured aminoglycosides, polymers, lipids, proteins, and nucleic acids, and carbohydrates (or saccharides) as major groups of biomolecules are explored in addition to silica-, iron-, silver-, and gold-based nanoparticles as carriers (Figure 2). Even carbon dots and quantum dots are subjected to the synthesis of aminoglycoside nanoparticles.

## 3. AMINOGLYCOSIDE-ENCAPSULATED POLYMERIC NANOPARTICLES

**3.1. Aminoglycoside-Loaded Carbohydrate-Supported Nanoparticles.** Biocompatible/biodegradable naturally occurring biomolecules and carbohydrates assist in the preparation of nanotherapeutics because of their chemically well-defined structure, protein repellency, high water solubility,

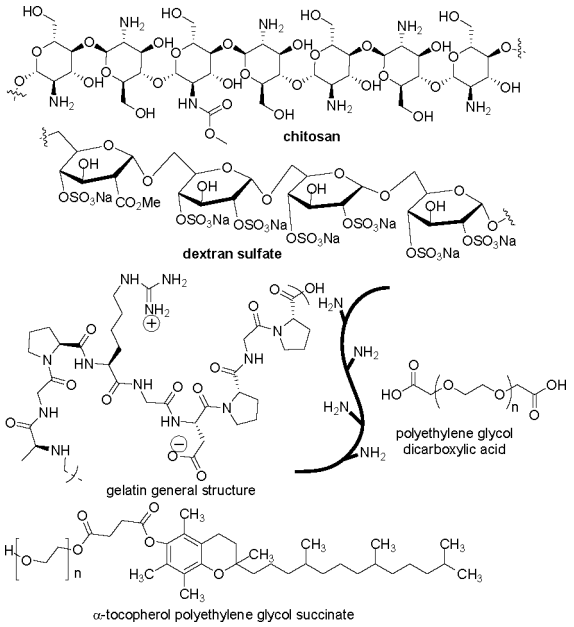


**Figure 2.** General structures of drug carriers.

and no aggregation properties.[5] An additional behavior of the carbohydrates is their ability to self-assemble to form polymeric nanoparticles, which encapsulate/load the AAs into nanostructured materials.

Strategies and reactions for the loading of aminoglycoside to chitosan nanoparticles based on the shielding of the polyanionic characteristic of dextran to the polycationic characteristic of aminoglycosides (Figure 3).[6a] For AA-loaded

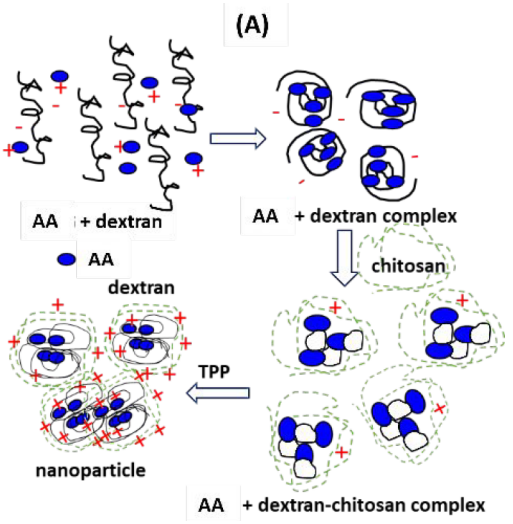


**Figure 3.** Diagram of the chitosan nanoparticle formation.

chitosan (CS) nanoparticles (NPs), the difference of drug, chitosan, and dextran sulfate concentrations varied the size of nanoparticles in the range of 492.23 to 779.37 nm, with positive zeta-potential. With the representative loading efficiency of tobramycin (37.2%), gentamicin (Gent), and streptomycin (SM) (~58 to 63%), in vitro, the nanoparticles sustain release >60% of drug into nanoparticles after 6 h in pH 1.2 buffer in a sustained behavior. Nano-SM has reduced bacilli growth by $p = 0.01$ in a mouse model infected with


https://doi.org/10.1021/acsomega.1c04399
ACS Omega 2022, 7, 4724−4734

*Mycobacterium tuberculosis* that was as good as subcutaneously injected aqueous streptomycin at the same dose (100 mg/kg). To crop more chitosan-based antibacterial films, Hari and colleagues[6b] assorted streptomycin-loaded starch nanoparticles (SS-NPs) with 1% chitosan and 1% gelatin, and SS-NPs improved the crystallinity and controlled swelling of the chitosan−gelatin film. These antimicrobial films inhibit *Escherichia coli* by approximately 90% and *Bacillus subtilis* by 80%, with a sustained release (60%) of streptomycin for 10 days, indicating its clinical potentiality through oral administration.

Deacon et al.[7a] accessed tobramycin-encapsulated alginate/chitosan nanostructures that resulted in uniform size distribution with 6:1.5:1.5 ratios of alginate, chitosan, and tobramycin, as determined by scanning electron microscopy (SEM) and dynamic light scattering (DLS) analysis. With 45% encapsulation efficiency, in vitro antimicrobial activity of the nanoparticles against *Pseudomonas aeruginosa* PA01 is similar to that of free tobramycin with a minimum inhibitory concentration (MIC) 0.625 mg/L. In the in vivo model for *P. aeruginosa* infection, the survival rate is found to be 90% upon injection of nanoparticles, inferring low nanoparticle toxicity. Tobramycin nanostructures removed the lethal inoculum caused by *P. aeruginosa* and doubled the survival rates compared to those with free tobramycin. Adapting the ethanol injection approach, Monteiro et al.[7b] prepared a chitosan nanofiber mesh (NFM) through the reaction of covalently immobilized SH groups of CS NFMs with liposomes. Gentamicin-loaded liposomes were formed with a 17% success rate (Figure 4). The random test indicated the

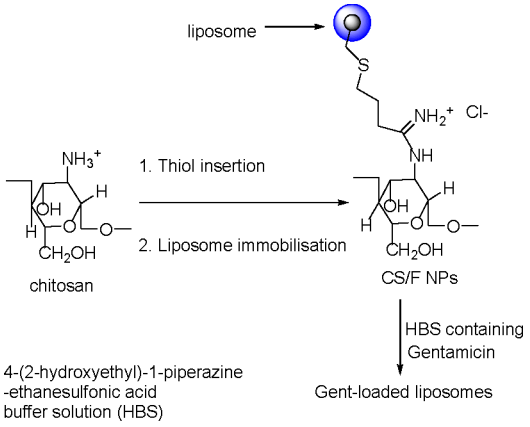


**Figure 4.** Attachment of liposomes with CS NFM and loading of gentamicin.

immobilization of liposomes (∼110 nm) on the surface of an electrospun CS nanofiber with a diameter between 100 and 500 nm. The preservation of electrospun CS NFMs and liposome structures was assigned from the SEM analysis of CS NFM before liposome immobilization and after liposome immobilization at the surface of an electrospun CS nanofiber. The drug−NPs displayed a sustained release of gentamicin during 16 h, accomplishing a steady state at 24 h. The released drug worked against *Staphylococcus aureus*, *E. coli*, and *P. aeruginosa*, with MICs 0.25, 0.83, and 0.50 mg/L, respectively, along with MBC 2.00 mg/L for all of the strains. Another example of chitosan/fucoidan nanoparticles (CS/F NPs) as carriers for gentamicin delivery was developed by Huang and co-workers.[8a] The gentamicin-loaded CS/F NPs (Gent-CS/F NPs) with a positive zeta-potential had an entrapment efficiency (EE) > 90%, higher than that of the reported values by Balmayor et al.[8b] from starch-conjugated CS NPs. Gent was encapsulated using the water/oil emulsion method (EEs from 55 to 67.2%), whereas for the tripolyphosphate cross-linked CS NPs, the EE of Gent loading was 61.7−87.2%.[8c] With sustained release for up to 72 h with 99% from biphasic CS/F NPs, the bacterial inhibition against *Klebsiella pneumoniae* by Gent-CS/F NPs (>96%) was lower than that of free Gent (after 48 h, 80−90%). The intratracheal injection of Gent-CS/F NPs (0.27 mg/kg) had an area under the concentration−time curve/MIC ratio higher than that of the intravenous administration of free Gent (0.5 mg/kg), showing the improvement of antibacterial efficacy.

**3.2. Aminoglycoside Antibiotic-Loaded PEG, PLGA, and TPGS Nanoparticles.** For nanoparticle formation with unique drug delivery properties, the biocompatible and biodegradable polymer poly(lactic acid-*co*-glycolic acid) (PLGA), which is hydrophilic, highly water-soluble, nonimmunogenic, and nontoxic, protein-resistant poly(ethylene glycol) (PEG), and water-soluble nonionic surfactant D-$\alpha$-tocopheryl polyethylene glycol 1000 succinate (TPGS) are used.

The kanamycin (KS) was encapsulated by the PEGylated water-soluble chitosan (WSC), that is, cationic deacetylated chitin NPs and PLGA-TPGS NPs. Interestingly, the KS-PEG-WSC NPs and KS-PLGA-TPGS NPs increased blood circulation while lowering dosage frequency.[9a] The WSC layer showed a significant impact on the surface load, and zeta-potential was reported to be near neutral at +3.61 mV. KS-PEG-WSC and KS-PLGA-TPGS NPs steadily and consistently released 91.56% in 14 days and 93.26% in 21 days, respectively.

For the transformation of injectable streptomycin to an oral version, streptomycin-encapsulated PLGA nanoparticles were made using the multiple emulsion technique.[9b] The average particle size of the drug-loaded NP was found to be 153.12 nm, and the drug encapsulation efficiency was observed as ±4.08% with 14.28 ± 0.83% drug loading. Streptomycin was maintained in plasma for 4 days and in organs for 7 days after a single oral dose of SM-PLGA nanoparticles was applied to mice. Regarding the relative bioavailability, encapsulated streptomycin was 21-fold higher than that of injectable drugs. In *M. tuberculosis* H37Rv-infected mice, eight doses of the weekly oral streptomycin-loaded NPs were equivalent to 24 free streptomycin intramuscular injections.

Likewise, Akhtar et al. designed intravenous gentamicin to oral absorption through encapsulation to PLGA nanoparticles modified with chitosan following water-in-oil-in-water formulations (w/o/w). The nanoformulation shows sustained release with increasing residence time to 11.22 ± 0.42 h and with the higher elimination half-life value (∼6.23 h).[10a] These particles were tested on plankton and biofilm crops of Gram-negative *P. aeruginosa* PA01 in vitro, as well as a peritoneal 96 h pattern of murine infections. With a MIC of 1.5 g/mL, free gentamicin inhibited bacterial growth, whereas the formulations of w/o/w and s/o/w (MIC of 3.0 g/mL) prevented the growth with efficacy lower than that of the free drug.

Gentamicin-AOT-loaded PLGA nanoparticles have a mean diameter ranging between 289.15 and 299.23 nm with a zeta-potential of −3.7 to 0.4 and −3.6 to 0.7 mV, respectively.[10b] In experimentally infected THP-1 monocytes, this gentamicin formulation reduced Gram-negative *Brucella melitensis* infection (>2-log10 reduction), whereas in vivo investigations


https://doi.org/10.1021/acsomega.1c04399
ACS Omega 2022, 7, 4724−4734

showed effectiveness in the liver and spleen for up to 4 days in infected mice. Even though 14 doses of free gentamicin had no effect on infection, only four doses of gentamicin-AOT-loaded nanoparticles reduced splenic infection by 3.23 log in 50% of infected mice without causing any adverse effects.

Abdelghany et al. developed a controlled release gentamicin formulation in water/oil/water and solid/oil/water using PLGA nanoparticles for treating *Pseudomonas* infections.[10c] Entrapment of a hydrophilic drug into a hydrophobic PLGA polymer can be increased by lowering the pH of the formulation, which reduces the hydrophilicity of the drug and thus improves entrapment, reaching levels up to 22.4 g/mg PLGA. These particles had a regulated release of gentamicin for up to 16 days under conventional incubation settings and have a MIC and MBC higher than that of free Gent.

Elfaky et al.[11a] reported the gentamicin loading on nanostructured lipid carriers (NLC) containing TPGS surfactant to protect from gentamicin-induced nephrotoxicity. In vivo studies with three groups of rabbits for 10 days revealed differences in plasma creatinine, urea, sodium, potassium, and calcium between the control and Gent-NLC materials considerably lower than those with gentamicin, confirming the protective effect on kidney function. Amikacin-loaded PLGA nanoparticles were synthesized[11b] by Sabaeifard et al. utilizing a solid-in-oil-in-water emulsion process with varied ratios of 50:50 PLGA/drug (100:3.5, 80:3.5, and 60:3.5) as well as a stabilizer (Pluronic F68) (0.5 or 1%). The drug encapsulation efficiency was 76.8%, and from the release kinetic study, 50% of the encapsulated drug was released within 1 h of incubation. No toxicity against RAW macrophages was observed in cell viability/cytotoxicity assays after 2 and 24 h of treatment. The slow-released drug from NPs showed activity 4 times lower than that of the free drug.

A synthetic block copolymer containing Pluronic-based core−shell nanostructures was synthesized by Ranjan and coworkers.[12a] With a 20% antibiotic loading in their formulation, the toxicity and adverse effects of this core−shell nanostructure encapsulating gentamicin, as well as the percentage of viable bacteria in the liver and spleen, were reduced. The anionic homo- and block copolymers of poly(ethylene oxide-*b*-sodium acrylate) (PEO-*b*-PAA$^-$Na$^+$) or poly(ethylene oxide-*b*-sodium methacrylate) (PEO-*b*-PMA$^-$Na$^+$) were blended with PAA$^-$Na$^+$-based polyanions to get stable nanoplexes at physiological pH following gentamicin encapsulation through electrostatic interactions (Figure 5).[12b] Gentamicin was also incorporated (at a rate of 26% by weight) into macromolecular complexes with an average diameter of 120 nm and a zeta-potential of −17 mV. These nanocomplexes can potentially enhance the attack of the intracellular pathogen *Salmonella*. The nephrotoxic profile of gentamicin nanoparticles was compared to that of free gentamicin by Jamshidzadeh et al.[12c] Furthermore, Mugabe and colleagues developed[12d] liposome-encapsulated gentamicin, which was less toxic than free gentamicin and showed high efficiency against dispersed *Salmonella* infections in mice. In rats and mice, the mean half-life of liposome-encapsulated gentamicin sulfate produced from egg phosphatidylcholine in serum was 4 times longer than that of free gentamicin in intravenous injection. This liposome encapsulation exhibited increased and extended activity in reticuloendothelial cells, particularly in the spleen and liver. In mice with acute septicemia, the liposomal formulation outperformed free medicines in terms of preventive activity.

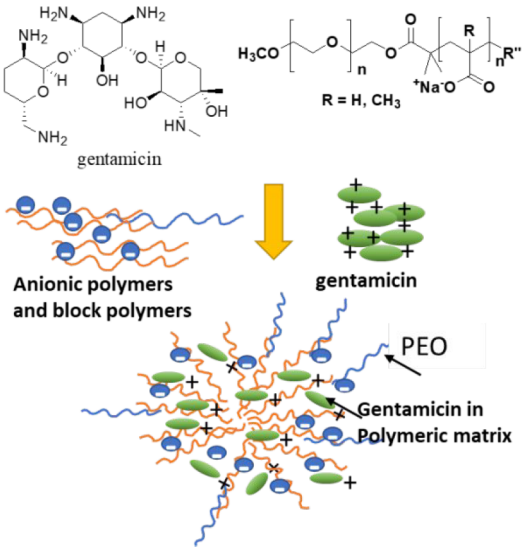


**Figure 5.** Gentamicin-loaded anionic homo- and block copolymers.

Conjugation of gentamicin to the hydrophobic block polymer POEGMA-*b*-PVBA containing aldehyde groups through Schiff base formation with gentamicin produced an amphiphilic block copolymer closely related to polyethylene glycol. Core cross-linked star polymers reacted with NO to form a polymer containing a *N*-diazeniumdiolate (NONOate) group that release NO in a regulated manner for a few days and formed dispersed biofilms. The DLS results showed a good polydispersity index (PDI 0.1) and a number-average size (15 nm) that agree well with the TEM data (Figure 6).

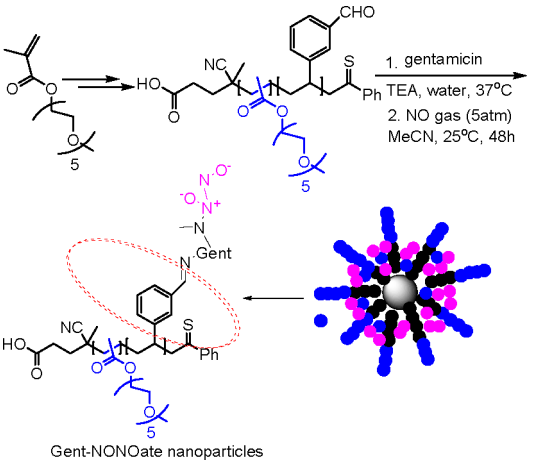


**Figure 6.** Synthesis of Gent-NONOate nanoparticles via RAFT polymerization.

According to Nguyen et al., the conjugate effectively reduced the viability of *P. aeruginosa* biofilms by more than 90 and 94% ($p < 0.0001$) in planktonic phases, respectively, compared to free gentamicin (at 10 mM, only 7 and 5% reduction).[13a]

Amphiphilic diblock copolymers comprising a hydrophilic PEG block and a hydrophobic block containing enzyme-cleavable self-immolative side linkages was investigated by Li and associates.[13b] After 4 h of penicillin G amidase (PGA) incubation, morphological changes of vesicles from transmission electron microscopy (TEM) analysis revealed the coexistence of PP2 LCVs with spherical nanoparticles, and in



https://doi.org/10.1021/acsomega.1c04399
ACS Omega 2022, 7, 4724−4734

the next 12 h, large compound vesicles (LCVs) were almost wiped out and formed hollow nanostructures, and after 24 h, only spherical nanoparticles remained. The released gentamicin from PGA-responsive large compound vesicle (PP2 LCV) bilayers against *P. aeruginosa* demonstrated the same growth inhibitory impact as free gentamicin at concentrations greater than 1.0 g/mL.

Self-polymerizable organic biopolymer, polydopamine (PDA), was tethered to gentamicin, kanamycin, and neomycin to obtain PDA−AA nanoconjugates under alkaline conditions (Tris buffer, pH 8.5) at 50 °C via Schiff base formation and Michael addition reaction (Figure 7).[14a] Out of these three

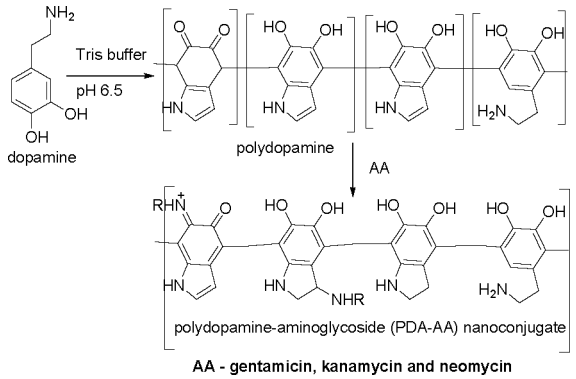


**Figure 7.** Structure of polydopamine−aminoglycoside nanoconjugates.

nanoconjugates, PDA−kanamycin was the most potent pathogen active and less toxic in human embryonic kidney cells (HEK293), although more toxic to human glioblastoma cells (U87). Nanoconjugates had antibacterial and anticancer effects greater than those of free drugs, although they were toxic to the cell line.

Ultrathin nanocapsules were prepared successfully by Majumdar[14b] upon coating of sodium alginate/polyallylamine hydrochloride (PAH) multilayers and loaded with gentamicin sulfate in the multilayer polyelectrolyte system to achieve a prolonged action of the drug. The average capsule size of the formulation was 400 nm, and the various parameters involved in the creation and optimization of the capsules were used. In capsular suspension, the maximal drug loading was reported to be 25.45% w/v (where 1.0 mL of capsular suspension contains 5000 capsules). In vitro, the total drug release was determined to be 65.91%. With each coating step, the capsule's zeta-potential alternates between −19.7 mV (Na-alginate) and +29.8 mV (PAH), indicating multilayered particle development.

**3.3. Aminoglycoside Antibiotic-Encapsulated Polymeric Nanogels.** Polymer matrices are hydrogels that swell but do not dissolve in water.[15a] Nanogels are nanoparticles made up of a hydrogel that has been physically or chemically cross-linked with hydrophilic polymer chains. Due to the tunable chemical and physical structure, good mechanical properties, biocompatibility, and high water content, these hydrogels have been extensively studied in the biomedical field.

Nanogels comprising polycationic chitosan and inorganic polyanion sodium tripolyphosphate was fabricated by Zabihian et al.[15b] The nanocarriers were homogeneous in distribution and had a considerable polydispersity index (0.3), with an average size of about 250 nm (unloaded) and 493 nm (gentamicin-loaded). The drug loading efficiency ranged between 28 and 32%, and Gent gradually and continuously released (∼90%) over 24 h. In MIC and potency testing, the antibacterial activity of gentamicin-loaded nanoparticles was not significantly diminished. The gentamicin's rapid burst release from nanogels unravelled the use of PVP as a physical "reinforcing agent".

## 4. SILICA NANOPARTICLES FOR AMINOGLYCOSIDE NANOHYBRIDS

In 2008, He and collaborators developed native $SiO_2$−gentamicin nanoparticles and gentamicin-loaded $SiO_2$ nanohybrids. The nanoparticles demonstrated the dose-dependent cell viability assay of SaOS-2 which is reduced both by $SiO_2$−gentamicin nanohybrids and native $SiO_2$ NPs in the cell counting kit-8 (CCK-8) assay.[16a] In the case of osteogenesis, the osteogenic differentiating capacity of SaOS-2 cells is not influenced by $SiO_2$−gentamicin nanohybrids or native $SiO_2$ NPs at a concentration range of 31.25−125 $\mu$g/mL and the concentrations of 9.65 $\mu$g/mL for free gentamicin.

An additional $SiO_2$−gentamicin nanohybrid for potential antimicrobial administration in orthopedic applications, developed by Mosselhy et al.,[16b] exhibited rapid release (21.4%) within the first 24 h and then 43.9% release in vitro in 5 days. This nanohybrid showed the most powerful antimicrobial activity against *B. subtilis* compared to that against *P. fluorescens* and *E. coli*. Filter-sterilized gentamicin has a MIC of 6.26 g/mL against *P. fluorescens* and *E. coli*, which is the quantity of gentamicin released from the 250 g/mL $SiO_2$−gentamicin nanohybrids. Free gentamicin-treated bacterial cells were completely deteriorated rather than bacterial cells treated with $SiO_2$−gentamicin nanohybrids, according to the TEM monographs.

Epoxy groups were introduced on the silica nanoparticles using 3-glycidyloxy propyl trimethoxysilane, followed by functionalization with gentamicin, neomycin, or kanamycin for the synthesis of aminoglycoside-conjugated silica nanoparticles (Figure 8) as described by Agnihotri et al.[16c] The attachment was measured by the increase in average size from 160 to 223 nm from native silica nanoparticles to epoxy−silica nanoparticles, which increased further following conjugation

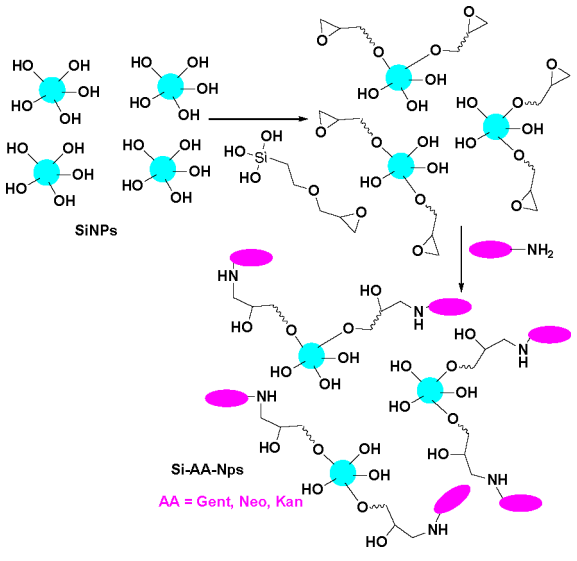


**Figure 8.** Structure of aminoglycoside-conjugated silica nanoparticles.



https://doi.org/10.1021/acsomega.1c04399
ACS Omega 2022, 7, 4724−4734

with aminoglycosides such gentamicin (256 nm), neomycin (298 nm), and kanamycin (269 nm). Limited cytotoxicity and antibacterial efficacy of functionalized silica NPs against Gram-positive and Gram-negative bacteria as well as kanamycin-resistant *E. coli* strain was found. Compared to native silica NPs, all the AA−silica nanoparticles showed significantly lower MICs but higher than that of free AAs. This may be attributable to the conjugation of aminoglycosides with active silica NPs in which a few primary amines are converted into secondary amines with charge density lower than that of primary amines.

## 5. AMINOGLYCOSIDE-COATED METAL NANOPARTICLES

**5.1. Aminoglycoside-Coated Iron Nanoparticles.** The synthesized magnetic nanoparticles (MNPs) prepared from coprecipitation of $Fe^{2+}$ and $Fe^{3+}$ iron salts in an alkali medium were coated with chitosan to form CS−MNPs, and subsequently, streptomycin was loaded to produce a strep-CS-MNP nanocomposite. X-ray diffraction was used to characterize CS−MNPs and nanocomposites. Later, the streptomycin-coated chitosan−magnetic (strep−CS−MNP) nanocomposite preparation[17a] was modified, and the permanent magnet was used to isolate strep−CS−MNP. Initially, the nanocomposite displayed a rapid release, but it became slower over time and reached 100% after 350 min, following the pseudo-second-order model for this release. The nanocomposite, strep−CS−MNP, exhibited antibacterial activity against methicillin-resistant *S. aureus* (MRSA). El-Say and El-Sawy highlighted in a separate paper that polymeric NPs, as opposed to metal-based NPs, have several advantages, including low toxicity, biocompatibility, biodegradability, and environmental friendliness. Tobramycin was delivered stably and effectively by binding to alginate that had been functionalized with DNase I before being encapsulated in chitosan NPs.[17b] Additionally, the antibacterial activity of the synthesized streptomycin-loaded chitosan-coated magnetic nanocomposites was assessed by El Zowalaty et al.[17c] (Figure 9).

Grumezescu et al.[18a] prepared a nanocarrier based on CS, poly(vinyl alcohol), and $Fe_3O_4$. Kanamycin was loaded into a water-dispersible metal oxide nanobiocomposite to increase active drug delivery, lowering the MIC of kanamycin by 2-fold (*S. aureus*) to 4-fold (*E. coli*) when compared to free kanamycin. The nanobiocomposite had a very minimal hazardous effect on eukaryotic cells in a cytotoxicity test.

Based on the electrostatic interactions of gentamicin with protonated chitosan and PEG (polyethylene glycol), Wang and colleagues[18b] studied the preparation of chitosan/$Fe_3O_4$@poly(ethylene glycol)−gentamicin NPs for drug entry through the bacterial membrane. PEG dicarboxylic acid was employed to improve the dispersity of $Fe_3O_4$ NP as it contains adequate carboxyl groups for binding. In an acidic environment, the CS and PEG of $Fe_3O_4$@PEG-Gent were protonated to impart a positive charge to the NP surface, facilitating interaction with the negatively charged bacterial cell membrane and displaying greater antibacterial activity over the free drug. Functionalized magnetic nanoparticles ($Fe_3O_4$@PEG-Gent) are biocompatible with normal cells and effective against planktonic bacteria and biofilms. These nanocomposites could penetrate the mature *S. aureus* biofilm with the help of a magnetic field due to the superparamagnetic properties of $Fe_3O_4$ NPs, leading to the successful delivery of gentamycin for biofilm eradication (Figure 10).

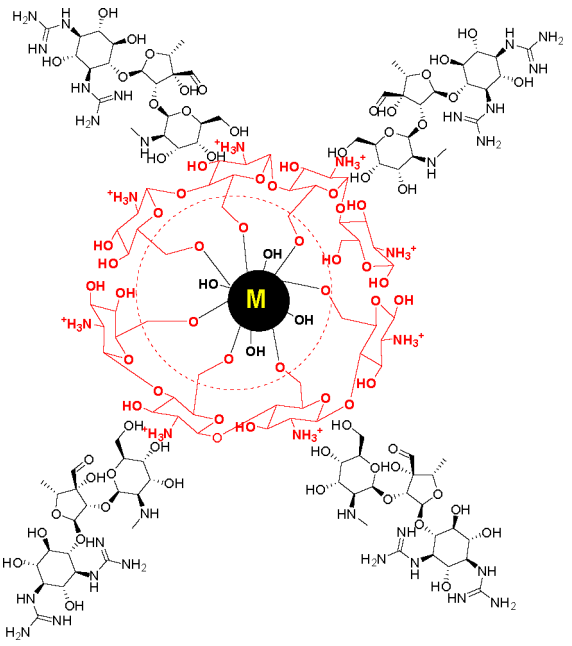


**Figure 9.** Chemical structure of the SM-coated nanocomposite.

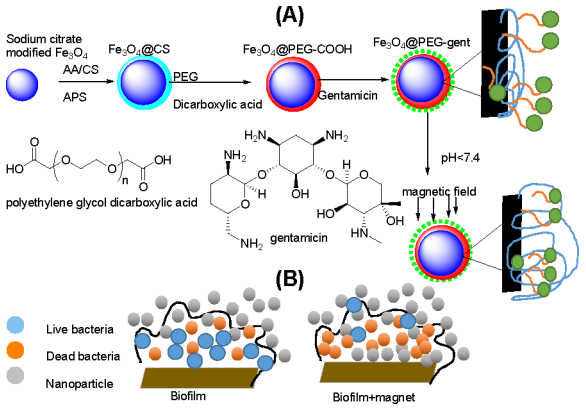


**Figure 10.** Schematic diagram of (A) $Fe_3O_4$@PEG-Gent nanoparticle formation. (B) Biofilms treated with $Fe_3O_4$@PEG-Gent nanoparticles in the absence and presence of a magnetic field.

**5.2. Aminoglycoside-Coated Silver Nanoparticles.** Caglayan and Onur devised a colorimetric silver nanoparticle sensor to determine aminoglycosides in milk.[19a] The yellow color of silver transformed into orange and red in proportion to the amounts of analytes. The decrease in absorbance of silver nanoparticles at 394 nm was used to conduct quantitative measurements of AAs in milk. Gentamicin, tobramycin, and amikacin have linear ranges of detection at 20−60, 23−60, and 60−100 ng/mL, respectively. AgNPs were also made by Ghodake et al.[19b] for colorimetric detection of aminoglycoside antibiotics in water, serum, and milk samples, with picomolar-level sensitivity to streptomycin.

Habash et al.[19c] explored tobramycin-loaded tiny citrate-coated silver NPs to inhibit the formation of *P. aeruginosa* biofilm, in which the NPs significantly increased the interaction of tobramycin with the cell membrane and biofilm. The synergistic effect of tobramycin activity was greater for smaller



https://doi.org/10.1021/acsomega.1c04399
ACS Omega 2022, 7, 4724−4734

AgNPs (10−20 nm) at inhibiting biofilms working through cellular membrane disruptions, according to minimum biofilm eradication concentration experiment using clinical *P. aeruginosa* isolates, and this synergistic effect is likely a strain-dependent phenomenon. Due to the synergism with the aminoglycoside capping agent, the produced silver NPs outperformed those capped with citrate or SDS in antibacterial activity against *E. coli* and *S. aureus*, according to Kora and Rastogi.[20a] The antibacterial and osteogenic properties of Gent-loaded AgNPs coated with silk fiber (SF) to address Ti-implant-associated infection and poor osseointegration issues were investigated by Zhou et al.[20b] In this study, the SF-based film was precomposed using two methods: dip-coating chitosan (DCS) and spin-coating chitosan (SCS) barrier layers. The antibacterial activity of the multilayer coating with the SCS layer was good, whereas the improvement in the DCS coating was restricted. Furthermore, the pH-dependent release behavior of the Ag and the bioactive SCS layer enriched adhesion, migration, and proliferation of preosteoblast MC3T3-E1 cells as well as osteoblast difference. Katva and collaborators[21a] presented that the combination of gentamicin and chloramphenicol with AgNPs has a superior antibacterial outcome in multi-drug-resistant *Enterococcus faecalis* compared to that with free antibiotics. Similarly, McShan et al.[21b] noticed the synergistic effect of neomycin with AgNPs with an enhanced antibacterial activity at concentrations below the MIC of either the NPs or the antibiotic and dose-dependent *Salmonella typhimurium* DT104 growth inhibition is observed for neomycin−AgNPs with $IC_{50}$ 0.43 $\mu$g/mL.

**5.3. Aminoglycoside Antibiotic-Coated Gold Nanoparticles.** Gold nanoparticles are widely acknowledged as attractive drug delivery possibilities because of their unique dimensions, varying surface functionalities, and regulated drug release.[22] The mixture of gold nanoparticles (AuNPs) and negative citrate ligands capped with polycationic ribostamycin aminoglycoside antibiotics showed unique properties.[22] The interaction between ribostamycin and AuNPs was examined at various doses using a combination of AuNPs of various sizes, and ribostamycin was determined using a dark-field optical microscopic study. Ribostamycin formed linear oligomers at higher concentrations, resulting in the formation of rod-like negative AuNPs. The antibacterial effect of ribostamycin, amikacin, and similar structural antibiotics may be directly related to the efficacy of the drug itself (Figure 11).

Wang et al.[23a] synthesized unmodified gold nanoparticles for a sensitive and selective colorimetric biosensor to detect gentamicin, amikacin, and tobramycin antibiotics in milk and pharmaceuticals. Rad and co-workers[23b] constructed gold nanoparticles coupled with aminoglycosides with a size of 10 nm to resist multi-drug-resistant, extensive drug resistance, and pan-drug-resistant bacteria. The antibacterial activity of the nanoconjugates of gentamicin and amikacin with gold against *Acinetobacter baumannii* isolates from burn wound infections was evaluated, and it was found that the conjugated amikacin had strong antibacterial activity (94.5%), whereas gentamicin had 50% efficacy. Payne et al.[23c] loaded the kanamycin on the surface of AuNPs, which enabled the delivery of cytosol and bactericidal to *S. epidermidis* and *Enterobacter aerogenes* to prevent robust growth of multi-drug-resistant bacteria. The one-step synthesis of capped KS-AuNPs has dose-dependent widespread antibacterial activity against Gram-positive, Gram-negative, and kanamycin-resistant bacteria, though KS-AuNPs have amplified toxicity to primate cell line bacteria (Vero 76). According to transmission electron microscopy and fluorescence microscopy, KS-AuNPs increased their effectiveness by disrupting the bacterial membrane, causing cytoplasmic leakage and cell death. In all of the bacteria tested, the MIC was significantly lower when compared to that of free kanamycin.

Roshmi et al.[24a] utilized *Bacillus* sp. SJ 14 (KJ451478) from the soil of jewelry sites for gold nanoparticle biosynthesis. The antibiotic-coated biogenic gold nanoparticles were tested against *S. epidermidis* 152 and vancomycin-bound AuNPs against *S. hemolyticus* 41, indicating that all AuNP-conjugated antibiotics had significantly lower MICs than their free forms, except for rifampicin-bound AuNPs. Mu and colleagues[24b] developed gold nanoparticles conjugated with chitosan−streptomycin (CS−SM), which easily passed through biofilm and cell membrane barriers, inhibiting biofilm formation, and eliminating *P. aeruginosa* preformed biofilm. It can kill both Gram-positive and Gram-negative bacteria (*Listeria monocytogenes*, *S. aureus*, *S. typhimurium*, and *E. coli*). After RAW264.7 cells were treated with the CS−SM conjugate and *L. monocytogenes* was visualized with fluorescence microscopy, there was a substantial reduction in the number of beneficial bacteria in a time-dependent manner (Figure 12).

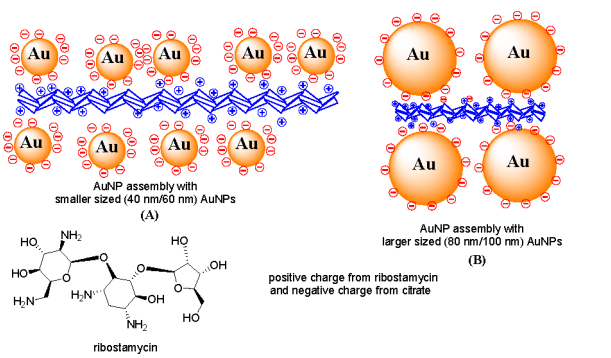


**Figure 11.** Interaction of self-assemble ribostamycin and citrate-capped AuNPs.

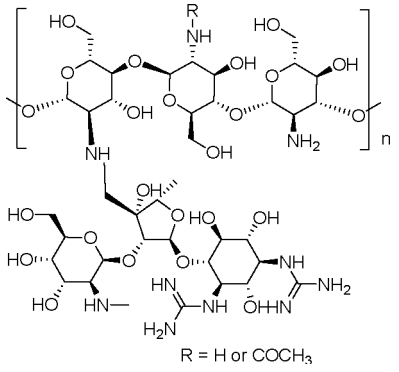


**Figure 12.** Chitosan−streptomycin conjugate.

In another experiment, CS−SM conjugates were produced for bacterial research. CS−SM-1 was formed by reduction of $HAuCl_4$ with $NaBH_4$ to form bare AuNPs, which were then mixed with CS, whereas CS−SM-2 was developed by chemical reduction of $HAuCl_4$/CS mixtures with sodium borohydride. They show $\lambda_{max}$ at 531 and 545 nm in their absorption spectra, respectively. According to DLS measurements, the sizes of


https://doi.org/10.1021/acsomega.1c04399
ACS Omega 2022, 7, 4724−4734

CS−SM-1 and CS−SM-2 were found to be 31 and 45 nm, with positive surface potentials of 18.7 and 25.0 mV, respectively. Bacterial TSB solutions (~$10^8$ CFU (colony-forming units)) were embedded in 96-well polystyrene microtiter plates to allow biofilm formation. These CS−SM NPs have retained their ability to kill 300 biofilms and prevent Gram-positive bacteria from forming biofilms. In a similar concentration, CS−SM NPs also had better bactericidal effects on both Gram-negative and Gram-positive bacteria when compared to those of the CS−SM conjugate or free streptomycin.[24c,d]

Per the report of Bhattacharya and colleagues,[25a] the conjugation of streptomycin and kanamycin to AuNPs enlarge the particle size of AuNPs, and according to the strength distribution plot, conjugated NPs are polydispersed, whereas the pure one is monodispersed. The MICs for drug conjugated AuNPs were significantly lower in all cases. Antibiotic stability improved as a result of the antibiotics' strong bond with AuNPs, which enhanced the antibiotics' bond energy. Nirmala Grace and Pandian confirmed amine group chelation of aminoglycosides with small AuNPs (15 nm).[25b] The development of the gold−drug complex was guided by the replacement of citrate with aminoglycosidic antibiotics. The TEM images indicated nanoparticle aggregation with an average size of 15−20 nm, and the color change and shift in plasmon absorption to longer wavelengths at 670 nm in the UV−vis spectrum also established the same. The antibacterial activities through growth inhibition of *S. aureus*, *Micrococcus luteus*, *E. coli*, and *P. aeruginosa* with drug-coated gold nanoparticles were higher than those of pure gold nanoparticles. The nanoparticles enhance the antibacterial activity against *E. coli*.

Ahangari et al.[26a] reported that gentamicin was conjugated onto AuNPs according to the method described by Huang. The color change from wine red to purple-blue of gold nanospheres of 10−12 nm diameter confirmed the conjugation. Biodistribution tests on BALB/c mice infected with *S. aureus* discovered that gentamicin-conjugated AuNPs were well retained in the bacterial infection site. The antibacterial activity of conjugated nanoparticles (0.09375 mg/mL) has more potential than free gentamicin (0.1875 mg/mL). To detect the kanamycin contamination in food, Sharma et al.[26b] developed a highly sensitive "turn-off/turn-on" biosensor using the intrinsic peroxidase-like activity of AuNPs. Saha et al.[26c] described the direct conjugation of streptomycin, kanamycin, and ampicillin to AuNPs. The TEM analysis revealed that the AuNPs conjugated to antibiotics produce larger particles. In SEM analysis, streptomycin conjugation has a rectangular rod shape, whereas kanamycin is stretched into star-like structures. For AuNP-conjugated streptomycin, the MICs were 7 and 14 μg/mL (50% reduction) and for kanamycin; these were 12 and 30 μg/mL (60% reduction) in *E. coli* DH5a.

## 6. QUANTUM-DOT-BASED NANOPARTICLES

Li et al.[27] synthesized a polyamine-functionalized carbon quantum dots (CQDs) by applying a hydrothermal treatment of citric acid and branched polyethylenimine with different molecular weights following attachment of gentamicin through carbonization (Figure 13). The high-resolution transmission electron microscopy revealed well-dispersed and narrow size distribution of particle with sizes ranging from 2.0 to 8.0 nm and a lattice spacing distance of 0.22 nm, which is like graphite (100) facets. The MICs of gentamicin sulfate-derived carbon

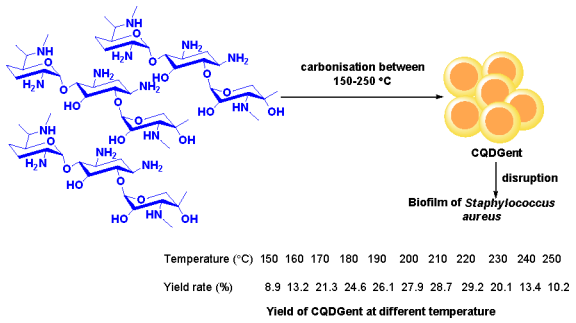


**Figure 13.** Gentamicin sulfate-derived carbon quantum dots.

quantum dots (CQD-Gents) by carbonization at 150 °C are almost similar to MIC of gentamicin against *S. aureus* (0.18 μg/mL) or *E. coli* (3 μg/mL), though above 190−200 °C, loss of antibacterial activity occurred. The toxicity of the synthesizing CQDs is low toward mammalian cells; even at a concentration of 2000 mg $mL^{-1}$, more than 91% of cells are viable, which is approximately 40000 times the MIC for *S. aureus*. After 10 min of treatment with CQD180, the cell morphology becomes irregular, and the bacterial membranes are destroyed in all directions, indicating the CQD180's ability to kill bacteria by disrupting their cell membranes, implying an additional mode of antibacterial action.

As a target to find bacterial biofilm, carbon dot PLGA-based hybrid nanoparticles (CQD-PLGA) as drug delivery systems were investigated by Huang et al.[28a] and processed with modulation of CQD content in the formulation applying microfluidic method. The TEM and DLS data indicate the narrow size distribution, and the size and zeta-potential are in the range of 100 to 150 nm and −20 to −50 mV, respectively. The drug loading into the CQD-PLGA was approximately 12−14%, and the encapsulated tobramycin delivered sustained release for up to ~72 h. The near-infrared radiation releases 55% of the drug during 7 h. The nanoparticles' good biocompatibility with eukaryotic cells and low cytotoxicity and the chemo-photothermal therapy against bacterial biofilms might be useful in a future application.

The amikacin conjugation with fluorescent carbon dot (CQDs@amikacin) nanoparticles was performed by applying hydrothermal carbonization of amikacin and diammonium hydrogen citrate. The synthesized CQDs@amikacin are uniformly dispersed. The average particle size ranges from 1.5 to 4 nm, and the maximum size of CQDs@amikacin is 2.5 nm. Chandra et al.[28b] have observed that there is no diffraction phase in the selected area electron diffraction pattern of CQDs@amikacin, conforming the particles as amorphous, and field-emission SEM images reveal its spherical morphology. The CQDs@amikacin detect *E. coli* in a linear range of $3.904 \times 10^5$ to $7.625 \times 10^2$ CFU/mL, with a detection limit of 552 CFU/mL, and here, amikacin works as a binding ligand toward *E. coli*. They also detect *E. coli* from apple juice, orange juice, and pineapple juice. Hence, this fluorescent carbon dot conjugated to amikacin might be used in the future to detect *E. coli* in other samples.

## 7. AMINOGLYCOSIDE-LOADED GRAPHENE

A new method by Pandey et al.[29] for the loading of gentamicin sulfate on a methanol-derived graphene (MDG) nanosheet was synthesized via the wet chemical route. At pH 3, the release of the drug was 62.75% following a diffusion-dominated


https://doi.org/10.1021/acsomega.1c04399
ACS Omega 2022, 7, 4724−4734

release mechanism. The X-ray diffraction analysis resulted in a broad peak at ∼26°, that is, close to the interplanar spacing of the close-packed planes in graphite (0.34 nm) in addition to a new peak arising at ∼11° (0.74 nm spacing). The drug-loaded graphene nanoplatform reduced *E. coli*'s growth, resulting in a viability loss of up to 82.2% compared to that with graphene alone (43.5% viability loss with 40 mg/mL). The gentamicin drug-loaded MDG nanomatrix demonstrated a strong antibacterial effect due to the synergistic effect of the drug and MDG. Furthermore, the controlled release provides a method for creating innovative graphene-based nanohybrids for the treatment of a variety of topical infections. Overall, the synthesis and bioactivities of the aminoglycoside-conjugated nanoparticles are summarized in Table S1.

## 8. CONCLUSIONS AND OUTLOOK

In this review article, we highlighted the research and studies on the preparation of nanostructured aminoglycoside antibiotics for future drug therapy. The use of nanoscale drug delivery devices is one of the burgeoning areas of research. Significant efforts continue in nanoparticle-based drug delivery that works via a similar mechanism of action; therefore, the research directions have moved toward the investigation of aminoglycosides to reduce toxicity, increase drug availability, and lower doses. Liposomes, lipids, carbohydrates, gold, silver, silicon, and other novel nanoparticle carriers are likely to play an important role in incorporating kanamycin, neomycin, streptomycin, gentamicin, and amikacin into the nanoparticles. Most of these AA-based nanoparticles are mainly studied in vitro, and a few are studied with in vivo assay; hence, more studies are essential for excellent clinical findings, particularly in terms of the lab to clinic transfer. We anticipate that the nanostructured aminoglycosides demonstrated by researchers around the world might escalate the development of new therapeutics.

## ■ ASSOCIATED CONTENT

### Supporting Information

The Supporting Information is available free of charge at https://pubs.acs.org/doi/10.1021/acsomega.1c04399.

Table S1 (PDF)

## ■ AUTHOR INFORMATION


### Corresponding Author

**Smritilekha Bera** − *School of Chemical Sciences, Central University of Gujarat, Gandhinagar 382030, India;* orcid.org/0000-0002-3213-5247; Email: lekha026@yahoo.com

### Author

**Dhananjoy Mondal** − *School of Chemical Sciences, Central University of Gujarat, Gandhinagar 382030, India*

Complete contact information is available at: https://pubs.acs.org/10.1021/acsomega.1c04399


### Notes

The authors declare no competing financial interest.

### Biographies

Dr. Smritilekha Bera earned her Ph.D. under the guidance of Dr. Mukund K. Gurjar at the National Chemical Laboratory in Pune, India. Dr. Bera began working as a DST scientist at the School of Chemical Sciences, Central University of Gujarat, India, after completing a three-year postdoctoral research associateship at the University of Manitoba in Canada and two years at the Rensselaer Polytechnic Institute (RPI) in New York. For several years, she has been researching the synthesis of natural products, heterocyclic building blocks, aminoglycosides, organic nanoparticles, and unnatural glycosaminoglycans (hyaluronan and chondroitin sulfate) for medicinal benefits. She has published 44 peer-reviewed articles, 6 book chapters, and 4 patents internationally over the years.

Dr. Dhananjoy Mondal is an assistant professor at the Central University of Gujarat's School of Chemical Sciences in Gandhinagar, India. He completed his postdoctoral research studies at the University of Winnipeg in Canada and Rensselaer Polytechnic Institute in the United States after getting his Ph.D. in synthetic organic chemistry from the National Chemical Laboratory in Pune, India. His research interests are on the synthesis of natural products, glycopeptidomimetics, and organo-nanocompounds for various biological applications. He has over 40 research articles and six book chapters to his credit.

## ■ ACKNOWLEDGMENTS

The authors acknowledge the infrastructure and support from the Central University of Gujarat.

## ■ REFERENCES


(1) (a) Burda, C.; Chen, X. B.; Narayanan, R.; El-Sayed, M. A. Chemistry and properties of nanocrystals of different shapes. *Chem. Rev.* **2005**, *105*, 1025−1102. (b) Biener, J.; Wittstock, A.; Baumann, T. F.; Weissmüller, J.; Bäumer, M.; Hamza, A. V. Surface chemistry in nanoscale. *Materials* **2009**, *2*, 2404−2428. (c) Gatoo, M. A.; Naseem, S.; Arfat, M. Y.; Mahmood Dar, A.; Qasim, K.; Zubair, S. Physicochemical Properties of Nanomaterials: Implication in associated toxic manifestations. *Bio. Med. Res. Int.* **2014**, *2014*, 8.

(2) (a) Yang, R.; Wei, T.; Goldberg, H.; Wang, W.; Cullion, K.; Kohane, D. S. Getting Drugs across Biological Barriers. *Adv. Mater.* **2017**, *29* (37), 1606596. (b) Blanco, E.; Shen, H.; Ferrari, M. Principles of nanoparticle design for overcoming biological barriers to drug delivery. *Nat. Biotechnol.* **2015**, *33* (9), 941−951.

(3) (a) Arya, D. P. *Aminoglycoside Antibiotics: From chemical biology to drug discovery*; Wiley: Hoboken, NJ, 2007. (b) Magnet, S.; Blanchard, J. S. Molecular insights into aminoglycoside action and resistance. *Chem. Rev.* **2005**, *105*, 477−497. (c) Review: Bera, S.; Mondal, D.; Palit, S.; Schweizer, F. Structural modifications of the neomycin class of aminoglycosides. *RSC Medicinal Chemistry* **2016**, *7*, 1499−1534. (d) Khan, F.; Pham, D. T. N.; Kim, Y. M. Alternative strategies for the application of aminoglycoside antibiotics against the biofilm-forming human pathogenic bacteria. *Appl. Microbiol. Biotechnol.* **2020**, *104*, 1955−1976. (e) Hu, J.; Yang, L.; Cheng, X.; Li, Y.; Cheng, Y. Aminoglycoside-Based Biomaterials: From Material Design to Antibacterial and Gene Delivery Applications. *Adv. Mater.* **2021**, *31*, 2103718.

(4) (a) Pelgrift, R. Y.; Friedman, A. J. Nanotechnology as a therapeutic tool to combat microbial resistance. *Adv. Drug Delivery Rev.* **2013**, *65*, 1803−15. (b) Abed, N.; Couvreur, P. Nanocarriers for antibiotics: A promising solution to treat intracellular bacterial infections. *Int. J. Antimicrob. Agents.* **2014**, *43*, 485−496.

(5) Kang, B.; Opatz, T.; Landfester, K.; Wurm, F. R. Carbohydrate nanocarriers in biomedical applications: functionalization and construction. *Chem. Soc. Rev.* **2015**, *44*, 8301−8325.

(6) (a) Lu, E.; Franzblau, S.; Onyuksel, H.; Popescu, C. Preparation of aminoglycoside-loaded chitosan nanoparticles using dextran sulphate as a counterion. *J. Microencapsul.* **2009**, *26*, 346−54. (b) Hari, N.; Jayakumaran Nair, A. Development and characterization of chitosan-based antimicrobial films incorporated with streptomycin loaded starch nanoparticles. *New Horiz. Transl. Med.* **2017**, *3*, 22−29.

(7) (a) Deacon, J.; Abdelghany, S. M.; Quinn, D. J.; Schmid, D.; Megaw, J.; Donnelly, R. F.; Jones, D. S.; Kissenpfennig, A.; Elborn, J.

S.; Gilmore, B. F.; Taggart, C.; Scott, C. J. Antimicrobial efficacy of tobramycin polymeric nanoparticles for Pseudomonas aeruginosa infections in cystic fibrosis: Formulation, characterisation and functionalisation with dornase alfa (DNase). *J. Controlled Release* **2015**, *198*, 55−61. (b) Monteiro, N.; Martins, M.; Martins, A.; Fonseca, N. A.; Moreira, J. N.; Reis, R. L.; Neves, N. M. Antibacterial activity of chitosan nanofiber meshes with liposomes immobilized releasing gentamicin. *Acta Biomaterial* **2015**, *18*, 196−205.

(8) (a) Huang, Y. C.; Li, R. Y.; Chen, J. Y.; Chen, J. K. Biphasic release of gentamicin from chitosan/fucoidan nanoparticles for pulmonary delivery. *Carbohydr. Polym.* **2016**, *138*, 114−22. (b) Balmayor, E. R.; Baran, E. T.; Azevedo, H. S.; Reis, R. L. Injectable biodegradable starch/chitosan delivery system for the sustained release of gentamicin to treat bone infections. *Carbohydr. Polym.* **2012**, *87*, 32−39. (c) Ji, J. G.; Hao, S. L.; Wu, D. J.; Huang, R.; Xu, Y. Preparation, characterization and *in vitro* release of chitosan nanoparticles loaded with gentamicin and salicylic acid. *Carbohydr. Polym.* **2011**, *85*, 803−808.

(9) (a) Mustafa, S.; Devi, V. K.; Pai, R. S. Kanamycin Sulphate Loaded PLGA-Vitamin-E-TPGS Long Circulating Nanoparticles Using Combined Coating of PEG and Water-Soluble Chitosan. *J. Drug Delivery* **2017**, *2017*, 1253294. (b) Pandey, R.; Khuller, G. K. Nanoparticle-based oral drug delivery system for an injectable antibiotic - streptomycin. Evaluation in a murine tuberculosis model. *Chemotherapy* **2007**, *53*, 437−41.

(10) (a) Akhtar, B.; Muhammad, F.; Aslam, B.; Saleemi, M. K.; Sharif, A. Pharmacokinetic profile of chitosan modified poly lactic co-glycolic acid biodegradable nanoparticles following oral delivery of gentamicin in rabbits. *Int. J. Biol. Macromol.* **2020**, *164*, 1493−1500. (b) Imbuluzqueta, E.; Gamazo, C.; Lana, H.; Campanero, M. Á.; Salas, D.; Gil, A. G.; Elizondo, E.; Ventosa, N.; Veciana, J.; Blanco-Prieto, M. J. Hydrophobic gentamicin-loaded nanoparticles are effective against *Brucella melitensis* infection in mice. *Antimicrob. Agents Chemother.* **2013**, *57*, 3326−3333. (c) Abdelghany, S. M.; Quinn, D. J.; Ingram, R. J.; Gilmore, B. F.; Donnelly, R. F.; Taggart, C. C.; Scott, C. J. Gentamicin-loaded nanoparticles show improved antimicrobial effects towards Pseudomonas aeruginosa infection. *Int. J. Nanomedicine.* **2012**, *7*, 4053−4063.

(11) (a) Elfaky, M. A.; Thabit, A. K.; Sirwi, A.; Fahmy, U. A.; Bahabri, R. M.; Al-Awad, E. A.; Basaeed, L. F. Development of a novel pharmaceutical formula of nanoparticle lipid carriers of gentamicin/ $\alpha$tocopherol and *In vivo* assessment of the antioxidant protective effect of $\alpha$-tocopherol in gentamicin-induced nephrotoxicity. *Antibiotics (Basel)* **2019**, *8*, 234. (b) Sabaeifard, P.; Abdi-Ali, A.; Soudi, M. R.; Gamazo, C.; Irache, J. M. Amikacin loaded PLGA nanoparticles against Pseudomonas aeruginosa. *European Journal of Pharmaceutical Sciences* **2016**, *93*, 392−398.

(12) (a) Ranjan, A.; Pothayee, N.; Seleem, M.; Jain, N.; Sriranganathan, N.; Riffle, J. S.; Kasimanickam, R. Drug Delivery using novel nanoplexes against a Salmonella mouse infection model. *J. Nanopart. Res.* **2010**, *12*, 905−914. (b) Ranjan, A. Antibacterial efficacy of core-shell nanostructures encapsulating gentamicin against an in vivo intracellular Salmonella model. *Int. J. Nanomedicine* **2009**, *4*, 289−297. (c) Jamshidzadeh, A.; Heidari, R.; Mohammadi-Samani, S.; Azarpira, N.; Najbi, A.; Jahani, P.; Abdoli, N. A comparison between the nephrotoxic profile of gentamicin and gentamicin nanoparticles in mice. *Biochem. Mol. Toxicol.* **2015**, *29*, 57−62. (d) Mugabe, C.; Halwani, M.; Azghani, A. O.; Lafrenie, R. M.; Omri, A. Mechanism of enhanced activity of liposome-entrapped aminoglycosides against resistant strains of Pseudomonas aeruginosa. *Antimicrob. Agents Chemother.* **2006**, *50*, 2016−2022.

(13) (a) Nguyen, T.-K.; Selvanayagam, R.; Ho, K. K.; Chen, R.; Kutty, S. K.; Rice, S. A.; Kumar, N.; Barraud, N.; Duong, H. T.; Boyer, C. *Chemical Science* **2016**, *7*, 1016−1027. (b) Li, Y.; Liu, G.; Wang, X.; Hu, J.; Liu, S. Enzyme-Responsive Polymeric Vesicles for Bacterial-Strain-Selective Delivery of Antimicrobial Agents. *Angew. Chem., Int. Ed.* **2016**, *55*, 1760−1764.

(14) (a) Singh, I.; Priyam, A.; Jha, D.; Dhawan, G.; Gautam, H. K.; Kumar, P. Polydopamine-aminoglycoside nanoconjugates: Synthesis, characterization, antimicrobial evaluation and cytocompatibility. *Materials Science and Engineering: C* **2020**, *107*, 110284. (b) Majumdar, A. J.; Parashar, A. K.; Jain, N. K.; Parashar, A. K. Ultrathin Multilayered Nanocapsules of Aminoglycoside for Topical Drug Delivery. *Curr. Res. Pharm. Sci.* **2012**, *03*, 171−176.

(15) (a) Oh, J.; Drumright, R. J.; Siegwart, D.; Matyjaszewski, K. The development of microgels/nanogels for drug delivery applications. *Prog. Polym. Sci.* **2008**, *33*, 448−477. (b) Zabihian, A.; Salouti, M.; Hamidi, M. Factorial design analysis and optimization of chitosan-based nanogels as controlled release system for gentamicin. *IET Nanobiotechnol* **2018**, *12*, 12−17.

(16) (a) He, W.; Mosselhy, D. A; Zheng, Y.; Feng, Q.; Li, X.; Yang, X.; Yue, L.; Hannula, S.-P. Effects of silica−gentamicin nanohybrids on osteogenic differentiation of human osteoblast-like SaOS-2 cells. *Int. J. Nanomed.* **2018**, *13*, 877−893. (b) Mosselhy, D.; Ge, Y.; Gasik, M.; Nordstrom, K.; Natri, O.; Hannula, S.-P. Silica-gentamicin nanohybrids: synthesis and antimicrobial action. *Materials* **2016**, *9* (3), 170. (c) Agnihotri, S.; Pathak, R.; Jha, D.; Roy, I.; Gautam, H. K.; Sharma, A. K.; Kumar, P. Synthesis and antimicrobial activity of aminoglycoside-conjugated silica nanoparticles against clinical and resistant bacteria. *New J. Chem.* **2015**, *39*, 6746.

(17) (a) El Zowalaty, M.; Webster, T. J; Zobir Hussein, M.; Ismail, M.; Hussein-Al-Ali, S. Synthesis, characterization, controlled release, and antibacterial studies of a novel streptomycin chitosan magnetic nanoantibiotic. *Int. J. Nanomedicine* **2014**, *9*, 549−557. (b) El-Say, K. M.; El-Sawy, H. S. Polymeric nanoparticles: promising platform for drug delivery. *Int. J. Pharm.* **2017**, *528*, 675−691. (c) El Zowalaty, M.; Hussein-Al-Ali, S.; Husseiny, M. I; Geilich, B.; Webster, T.; Hussein, M. Z. The ability of streptomycin-loaded chitosan-coated magnetic nanocomposites to possess antimicrobial and antituberculosis activities. *Int. J. Nanomedicine* **2015**, *10*, 3269−74.

(18) (a) Grumezescu, M.; Holban, A. M.; Andronescu, E.; Ficai, A.; Bleotu, C.; Carmen, C. M. Water dispersible metal oxide nano-biocomposite as a potentiator of the antimicrobial activity of kanamycin. *Letters in Applied Nano BioScience* **2012**, *1*, 77−82. (b) Wang, X.; Deng, A.; Cao, W.; Li, Q.; Wang, L.; Zhou, J.; Hu, B.; Xing, X. Synthesis of chitosan/poly (ethylene glycol)-modified magnetic nanoparticles for antibiotic delivery and their enhanced anti-biofilm activity in the presence of magnetic field. *J. Mater. Sci.* **2018**, *53*, 6433−6449.

(19) (a) Caglayan, M. G.; Onur, F. Silver nanoparticle-based analysis of aminoglycosides. *Spectrosc. Lett.* **2014**, *47*, 771−780. (b) Ghodake, G.; Shinde, S.; Saratale, R. G.; Kadam, A.; Saratale, G. D.; Syed, A.; Marraiki, N.; Elgorban, A. M.; Kim, D. Y. Silver nanoparticle probe for colorimetric detection of aminoglycoside antibiotics: picomolar-level sensitivity toward streptomycin in water, serum, and milk samples. *Journal of the Science of Food and Agriculture* **2020**, *100*, 874−884. (c) Habash, M. B.; Goodyear, M. C.; Park, A. J.; Surette, M. D.; Vis, E. C.; Harris, R. J.; Khursigara, C. M. Potentiation of tobramycin by silver nanoparticles against Pseudomonas aeruginosa biofilms. *Antimicrob. Agents Chemother.* **2017**, *61* (11), e00415-17.

(20) (a) Kora, A. J.; Rastogi, L. Enhancement of antibacterial activity of capped silver nanoparticles in combination with antibiotics, on model gram-negative and gram-positive bacteria. *Bioinorg. Chem. Appl.* **2013**, *2013*, 871097. (b) Zhou, W.; Li, Y.; Yan, J.; Xiong, P.; Li, Q.; Cheng, Y.; Zheng, Y. Construction of self-defensive antibacterial and osteogenic AgNPs/gentamicin coatings with chitosan as nanovalves for controlled release. *Sci. Rep.* **2018**, *8*, 13432.

(21) (a) Katva, S.; Das, S.; Moti, H. S.; Jyoti, A.; Kaushik, S. Antibacterial synergy of silver nanoparticles with gentamicin and chloramphenicol against *Enterococcus faecalis*. *Pharmacogn. Mag.* **2018**, *13*, S828−S833. (b) McShan, D.; Zhang, Y.; Deng, H.; Ray, P. C.; Yu, H. Synergistic antibacterial effect of silver nanoparticles combined with ineffective antibiotics on drug resistant *Salmonella typhimurium* DT104. *J. Environ. Sci. Heal. Part C* **2015**, *33*, 369−384.

(22) Zheng, T.; Li Sip, Y. Y.; Leong, M. B.; Huo, Q. Linear self-assembly formation between gold nanoparticles and aminoglycoside antibiotics. *Colloids Surf., B* **2018**, *164*, 185−191.



https://doi.org/10.1021/acsomega.1c04399
*ACS Omega* 2022, 7, 4724−4734

(23) (a) Wang, R.; Fan, S.; Wang, R.; Wang, R.; Dou, H.; Wang, L. Determination of aminoglycoside antibiotics by a colorimetric method based on the aggregation of gold nanoparticles. *Nano* **2013**, *8*, 1350037. (b) Rad, M. R.; Kazemian, H.; Yazdani, F.; Monfared, M. R. Z.; Rahdar, H.; Javadi, A.; Kodori, M. Antibacterial activity of gold nanoparticles conjugated by aminoglycosides against A. Baumannii isolates from burn patients. *Recent Pat. Antiinfect. Drug Discovery* **2019**, *13*, 256−264. (c) Payne, J. N.; Waghwani, H. K.; Connor, M. G.; Hamilton, W.; Tockstein, S.; Moolani, H.; Chavda, F.; Badwaik, V.; Lawrenz, M. B.; Dakshinamurthy, R. Novel synthesis of kanamycin conjugated gold nanoparticles with potent antibacterial activity. *Front. Microbiol.* **2016**, *7*, 607.

(24) (a) Roshmi, T.; Soumya, K. R.; Jyothis, M.; Radhakrishnan, E. K. Effect of biofabricated gold nanoparticle-based antibiotic conjugates on minimum inhibitory concentration of bacterial isolates of clinical origin. *Gold Bull.* **2015**, *48*, 63−71. (b) Mu, H.; Tang, J.; Liu, Q.; Sun, C.; Wang, T.; Duan, J. Potent antibacterial nanoparticles against biofilm and intracellur Bacteria. *Sci. Rep.* **2016**, *6*, 18877. (c) Mu, H.; Liu, Q.; Niu, H.; Sun, Y.; Duan, J. Gold nanoparticles make chitosan−streptomycin conjugates effective towards Gram-negative bacterial biofilm. *RSC. Adv.* **2016**, *6*, 8714−8721. (d) Mu, H.; Niu, H.; Wang, D.; Sun, F.; Sun, Y.; Duan, J. Chitosan conjugation enables intracellular bacteria susceptible to aminoglycoside antibiotic. *Glycobiol* **2016**, *26*, 1190−1197.

(25) (a) Bhattacharya, D.; Saha, B.; Mukherjee, A.; Ranjan Santra, C.; Karmakar, P. Gold nanoparticles conjugated antibiotics: stability and functional evaluation. *Nanosci. Nanotechnol.* **2012**, *2*, 14−21. (b) Nirmala Grace, A.; Pandian, K. Antibacterial efficacy of aminoglycosidic antibiotics protected gold nanoparticles-A brief study. *Colloids Surf. A Physicochem. Eng. Asp.* **2007**, *297*, 63−70.

(26) (a) Ahangari, A.; Salouti, M.; Heidari, Z.; Kazemizadeh, A. R.; Safari, A. A. Development of gentamicin-gold nanospheres for antimicrobial drug delivery to Staphylococcal infected foci. *Drug delivery* **2013**, *20*, 34−39. (b) Sharma, T. K.; Ramanathan, R.; Weerathunge, P.; Mohammadtaheri, M.; Daima, H. K.; Shukla, R.; Bansal, V. Aptamer-mediated 'turn-off/turn-on' nanozyme activity of gold nanoparticles for kanamycin detection. *Chem. Commun.* **2014**, *50*, 15856−15859. (c) Saha, B.; Bhattacharya, J.; Mukherjee, A.; Ghosh, A.; Santra, C.; Dasgupta, A.; Karmakar, P. In vitro structural and functional evaluation of gold nanoparticles conjugated antibiotics. *Nanoscale Res. Lett.* **2007**, *2*, 614−622.

(27) (a) Li, P.; Yang, X.; Zhang, X.; Pan, J.; Tang, W.; Cao, W.; Zhou, J.; Gong, X.; Xing, X. Surface chemistry-dependent antibacterial and antibiofilm activities of polyamine-functionalized carbon quantum dots. *J. Mater. Sci.* **2020**, *55*, 16744−16757. (b) Li, P.; Liu, S.; Cao, W.; Zhang, G.; Yang, X.; Gong, X.; Xing, X. Low-toxicity carbon quantum dots derived from gentamicin sulfate to combat antibiotic resistance and eradicate mature biofilms. *Chem. Commun.* **2020**, *56*, 2316−2319.

(28) (a) Huang, Z.; Zhou, T.; Yuan, Y.; Natalie Kłodzinska, S.; Zheng, T.; Sternberg, C.; Mørck Nielsen, H.; Sun, Y.; Wan, F. Synthesis of carbon quantum dot-poly lactic-co-glycolic acid hybrid nanoparticles for chemo-photothermal therapy against bacterial biofilms. *J. Colloid Interface Sci.* **2020**, *577*, 66−74. (b) Chandra, S.; Chowdhuri, A. R.; Mahto, T. K.; Samui, A.; Sahu, S. K. One-step synthesis of amikacin modified fluorescent carbon dots for the detection of Gram-negative bacteria like Escherichia coli. *RSC Adv.* **2016**, *6*, 72471−72478.

(29) (a) Pandey, H.; Parashar, V.; Parashar, R.; Prakash, R.; Ramteke, P. W.; Pandey, A. C. Controlled drug release characteristics and enhanced antibacterial effect of graphene nanosheets containing gentamicin sulfate. *Nanoscale* **2011**, *3*, 4104−4108. (b) Parashar, V.; Kumar, K.; Prakash, R.; Pandey, S. K.; Pandey, A. C. Methanol derived large scale chemical synthesis of brightly fluorescent graphene. *J. Mater. Chem.* **2011**, *21*, 6506−6509.



https://doi.org/10.1021/acsomega.1c04399
*ACS Omega* 2022, 7, 4724−4734